Since January 2020 Elsevier has created a COVID-19 resource centre with free information in English and Mandarin on the novel coronavirus COVID-19. The COVID-19 resource centre is hosted on Elsevier Connect, the company's public news and information website.

Journal of Molecular Structure 1272 (2023) 134160

Contents lists available at ScienceDirect

Journal of Molecular Structure

journal homepage: www.elsevier.com/locate/molstr

Rational design of an anti-cancer peptide inhibiting CD147 / Cyp A interaction

Zahra Maani[a], Safar Farajnia[b], Leila Rahbarnia[c,*], Elaheh Zadeh Hosseingholi[a,*], Nazli Khajehnasiri[d], Parisa Mansouri[d]

[a] Department of Cellular and Molecular Biology, Faculty of Science Faculty, Azarbaijan Shahid Madani University, Tabriz, Iran
[b] Drug Applied Research Center, Tabriz University of Medical Sciences, Tabriz, Iran
[c] Infectious and Tropical Diseases Research Center, Tabriz University of Medical Sciences, Tabriz, Iran
[d] Higher Education Institute of Rab-Rashid, Tabriz, Iran

ARTICLE INFO

Article history:
Received 22 June 2022
Revised 27 August 2022
Accepted 13 September 2022
Available online 16 September 2022

Keywords:
Melittin
TAT peptide
Molecular dynamic simulations
Coarse-grained simulations
Anticancer activity
anti-COVID19

ABSTRACT

The CD147 / Cyp A interaction is a critical pathway in cancer types and an essential factor in entering the COVID-19 virus into the host cell. Melittin acts as an inhibitory peptide in cancer types by blocking the CD147/ Cyp A interaction. The clinical application of Melittin is limited due to weak penetration into cancer cells. TAT is an arginine-rich peptide with high penetration ability into cells widely used in drug delivery systems. This study aimed to design a hybrid peptide derived from Melittin and TAT to inhibit CD147 /Cyp A interaction. An amino acid region with high anti-cancer activity in Melittin was selected based on the physicochemical properties. Based on the results, a truncated Melittin peptide with 15 amino acids by the GGGS linker was fused to a TAT peptide (nine amino acids) to increase the penetration rate into the cell. A new hybrid peptide analog(TM) was selected by replacing the glycine with serine based on random point mutation. Docking results indicated that the TM peptide acts as an inhibitory peptide with high binding energy when interacting with CD147 and the CypA proteins. RMSD and RMSF results confirmed the high stability of the TM peptide in interaction with CD147. Also, the coarse-grained simulation showed the penetration potential of TM peptide into the DOPS-DOPC model membrane. Our findings indicated that the designed multifunctional peptide could be an attractive therapeutic candidate to halter tumor types and COVID-19 infection.

1. Introduction

Anticancer peptides (ACPs) are promising therapeutic agents due to their high penetration, toxicity, and ease of modification. Anticancer peptides can destroy cancer cells through necrosis and apoptosis by pore formation or membrane lysis [1]. Melittin, a small peptide with 26 amino acids (GIGAVLKVLTTGLPALISWIKRKRQQ), was first obtained from bee venom [2]. Until now, several biological properties including antimicrobial, anti-radiation, anti-inflammatory, anti-arthritic, anti-tumor, and anti-AIDS has been confirmed for Melittin [3–6]. However, there are some limitations in the clinical application of Melittin, including high toxicity (mainly hemolytic activity), influence on gene expression, and genotoxicity [7–9]. One of the main factors involved in Melittin's anticancer activity is blocking matrix metalloproteinase (MMPs) pathway and inhibiting caspase activity [10–12]. Based on studies, a high expression of MMPs has been detected in a wide range of cancer cells such as malignant bladder tumor, Cutaneous squamous cell carcinoma (SCC), and breast cancer [13]. The expression of MMPs is induced through interaction between by CD147 cell-surface receptor, a transmembrane glycoprotein with cyclophilin A (CypA) [14]. Hence, intervention in the interaction between CD147 and CypA through an inhibitory peptide may be attractive for inhibiting the MMP expression and inducing the caspase pathway. On the other hand, studies highlight the critical role of the CypA/CD147 interaction in the capability of the SARS-CoV-2 virus to enter the host cells; hence inhibiting this interaction may be an attractive approach to controlling COVID infection [15]. According to studies, Melittin as an anticancer agent can downregulate MMP-9 and CD147 via inhibiting the expression of CypA. However, its clinical application can be limited because of its low penetration into solid tumors. In recent years, several analogs of Melittin have been constructed to improve the biological activity against

Abbreviations: ACPs, Anticancer peptides; M, melittin; GRAVY index, the sum of the hydropathy values; TM, TAT-Melittin; H, mean hydrophobicity; μH, the hydrophobic moment; z, net charge; NPT, constant pressure; NVT, constant volume; RMSF, root-mean-square fluctuations; RMSD, root-mean-square deviation.

* Corresponding author.
E-mail address: zhosseingholi@azaruniv.edu (E.Z. Hosseingholi).

https://doi.org/10.1016/j.molstruc.2022.134160
0022-2860/

cancer types [10,13,16]. However, there is no FDA-approved drug-based Melittin for clinical use [17].

HIV-1 TAT is a cell-penetrating peptide widely used to deliver different therapeutic molecules into cells [18]. A cell-transmitting region with nine amino acids (RKKRRQRRR) in TAT peptide acts as a cell-penetrating peptide [19]. The ability of TAT intracellular penetration is related to the high density of positive charges in its sequence [20]. This study designed a dual hybrid peptide derived from Melittin to inhibit the entry of the COVID virus and to control cancer types through more penetration potential into solid tumors via blocking the CypA/CD147 interaction by bioinformatics tools and molecular dynamic (MD) simulation studies.

2. Material

2.1. Design, physicochemical properties, and structure prediction of polypeptides

Several databases, including the UniProt database (https://www.uniprot.org) and APD (https://pubmed.ncbi.nlm.nih.gov/14681488/) and PDB databases (https://www.rcsb.org/), were used for the extraction and evaluation of physicochemical properties (molecular weight, net charge, instability index) of Melittin and TAT peptides. The secondary structure of proteins was predicted by SWISS-MODEL (https://swissmodel.expasy.org). PEP-FOLD (https://bioserv.rpbs.univ-paris-diderot.fr/services/PEP-FOLD/) and QMEAN server (https://swissmodel.expasy.org/qmean/) were used to predict peptide secondary structure. Pymol software was utilized for the visualization of peptide analogs.

2.2. The examination of inhibitory property of Melittin in interaction with CD147 receptor

Based on the previous studies, Melittin acts as an inhibitory peptide to disrupt the interaction between CD147 and Cyp A through binding to proline 211 of CD147 [21–24]. To design a hybrid peptide resulting from the fusion of Melittin and TAT, maintaining the function of Melittin as an inhibitory peptide is essential. For analysis of the binding region of Melittin to CD147, the sequences of CD147 and CypA were extracted from the PDB database, and the secondary structure of CD147 and CypA proteins was predicted based on modeling done by SWISS-MODEL and Qmean servers. Subsequently, Cluspro2.0 docking (https://cluspro.bu.edu/login.php) was performed to assess the binding region Melittin to CD147 and was displayed by pymol software.

2.3. Hybrid peptide design

The specific region of Melittin with anticancer property (GLPALISWIKRKRQQ) was selected for binding to the nine amino acid sequence of TAT (RKKRRQRRR) with high penetrating ability into the cell. For this, a flexible linker was needed to fuse two peptides. Several linkers were selected, including GSG, GGS, AGP, GGGSGGGS, GSGGSG, and GGGS, based on their application in the construction of hybrid peptides [25,26]. Each linker was used in the hybrid peptide design, and the secondary structure of the peptides was predicted by PEP-FOLD, SWISS-MODEL, and QMEAN servers. The interaction of new hybrid peptides with CD147 was evaluated by Clus Pro 2.0 server to examine the specific binding of the peptide to proline 211 in CD147. Results were visualized by pymol software. After selecting a suitable linker, new hybrid peptide analogs were produced by the AntiCP server by inducing point mutations in the hybrid peptide sequence. The best peptide analog was selected based on the highest SVM score. In this stage, the interaction between analogs with CD147 was again examined by Clus Pro 2.0.

2.4. Anticancer ability and solubility analysis of designed peptide

For the prediction of anticancer activity of the designed peptide, the ENNAACT web server (https://research.timmons.eu/ennaact) was used. The peptide sequence was uploaded in FASTA format and evaluated for anticancer property based on the calculated score. The solubility of the designed peptide was investigated using the protein-sol web server (https://protein-sol.manchester.ac.uk).

2.5. Molecular dynamics (MD) simulation

MD simulation was conducted to analyze the stability of the CD147 / CypA complex and the interaction between the inhibitory peptide designed with CD147 protein. Docking results of CD147 with Cyp A were entered into GROMACS 4.6.5 software as a PDB file. The protein structures were centered in a cubic box and filled with water molecules using the SPC water model [27] and expanded up to 10 Å from solute atoms to any edge of the cubic box. NaCl ions with a concentration of 100 mM were used as neutralizing agents, and an appropriate number of Na+ and Cl- ions were added to all simulations. Energy minimization for the whole system was performed as the steepest descent to eliminate the undesirable contacts between the solvent and target molecules. NPT (constant pressure) and NVT (constant volume) ensemble conditions were performed at 310°K for 100 PS to equilibrate the minimized systems. The peptide's root-mean-square fluctuations (RMSF) and root-mean-square deviation (RMSD) were calculated coupled with the MD trajectories. The Parrinello-Rahman algorithm set the pressure of 1 bar under isotropic conditions. Electrostatic interactions were calculated by PME [28] and the LINCS procedure to impose all bonds involving hydrogen atoms [29]. After the neutralization stage, the energy minimization was also conducted during the steepest descent algorithm. MD equilibration was done for 100 PS with positional restraints on protein-heavy atoms with a spring constant of 1000 kcal.mol-1nm-2 to avoid the non-physical conformational change of the solvated protein. The Final MD simulation was run without restraint for 100 ns. RMSD was calculated to examine protein changes during MD simulation. RMSF was calculated to detect the fluctuation of protein residues over time from a reference position during simulation. Molecular Mechanics/Poisson–Boltzmann Surface Area (MM/PBSA) method was used for calculating binding free energy from MD trajectory [30,31].

2.6. Coarse-grained (CG) MD simulation

CG-MD simulation is an attractive tool for analyzing the interaction between cell-penetrating peptides and biomembranes [32].

This study conducted CG-MD simulations based on the hybrid peptide interaction with the DOPS-DOPC membrane (DOPS and DOPC, molar ratio 2/8) using the GROMACS software package. The peptide/lipid (P/L) ratio was equal to 1/25, so that 8 peptides were used for every 200 lipids. The configuration was started using packmol software in a cubic box with a 25 nm edge in each dimension. The MARTINI force field [25] was utilized for 1500 ns simulations. All-atom peptide structure was converted to CG model using martinize.py python script. The martini22 force field was used in model generation. Afterward, the peptide (CG model) and membrane (CG model) interaction were simulated using gromacs software.

The peptide molecules were added to the CG system with a molar ratio of about 0.01. The system was filled with the coarse-grained water model, and 80 Na+ ions were added to the box to neutralize the system. A reference pressure equal to 1 bar was applied using a Parrinello–Rahman barostat. The energy was minimized during 1000 steps and equilibrated in an NVT ensemble

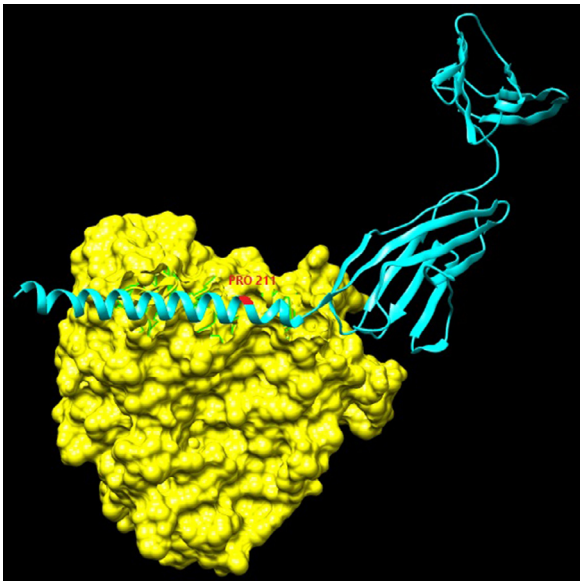

Fig. 1. Interaction between CD147 and CypA proteins based on ClusPro 2.0 docking. The blue, yellow and red colors are related to CD147, CypA proteins and proline 211.

at 310° K. GC simulation was conducted for 1500 ns simulation. The hydrophobicity of the peptide was evaluated using ExPASy: ProtScale tool.

3. Results

3.1. The design of a hybrid peptide

Based on the physicochemical properties of Melittin (GIGAVLKVLTTGLPALISWIKRKRQQG), an amino acid region (GLPALISWIKRKRQQ) with high anticancer activity was selected, and also nine amino acids from the Tat sequence (MEPVDPRLEPWKHPGSQPKTACTSCYCKRCCFHCQVCFITKGLGISYGRKKRRQRRRADQDSQNHQVSLSKQPTSQPRGDPTGPKESKKEVERETTTDPGDQWMAS) was selected based on previous studies regarding high permeability into cell membrane [26,33].

3.2. The selection of a suitable linker

Six hybrid peptides were constructed using six selected linkers and analyzed by AntiCP server and ClusPro docking for interaction with CD147 protein. The CD147 /CypA interaction in proline 211 was confirmed by Clus pro docking (Fig. 1). For this, the 3D structure of CD147 and hybrid peptides were made, and Clus pro docking was performed. The crystal structure of CD147 (PDB id: 3B5H) related to the extracellular portion of this protein was used for docking based on previous studies [34, 35]. The best construct was selected based on binding CD147 through proline 211 to the hybrid peptide. Among six hybrid peptides designed, only one (GLPALISWIKRKRQQ**GGGS**RKKRRQRRR) indicated specific binding in a defined location (proline 211) by fusing Melittin and TAT sequences by a GGGS linker (Fig. 2) with SVM score: of 0.67.

3.3. Optimization of the hybrid peptide through inducing point mutations

In the next step, the AntiCP server was used to make novel analogs of hybrid peptide with higher anticancer properties by induction point mutations. The best analogs were selected based on the SVM score (Table 1). The new analogs with the highest score

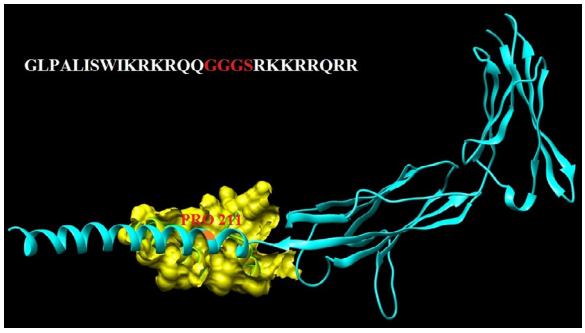

Fig. 2. Clus Pro 2.0 docking results related to the construction of the hybrid peptide designed by the best linker. The blue, yellow and red colors are related to CD147 protein, peptide and the binding site (proline 211).

were examined by cluspro docking to detect binding sites between CD147 and peptide.

According to the results, a hybrid peptide with alteration of the first amino acid (Glycine) to (Serine) amino acid with SVM: 0.82 was selected, and the specific binding was confirmed by cluspro docking. The final peptide sequence (TM) was as follows:(**S**LPALISWIKRKRQQ**GGGS**RKKRRQRRR) (Fig. 3). The anticancer property of TM was confirmed by the ENNAACT server (https://research.timmons.eu/ennaact).

3.4. Evaluation of peptide solubility

Based on the results, the solubility of the designed peptide was equal to 0.729, which was higher than the solubility score determined by the server for control mode (0.45). Hence, the TM peptide can have high solubility (Fig. 4).

3.5. MD simulation results

The binding energy and interaction between CD147 and Cyp A proteins and the TM peptide with CD147 were examined by MD simulation. The RMSD values indicated a range of 0.4 to 3 nm during simulation for the CD147/CypA complex, which was stabilized after 70 ns without undesired fluctuation (Fig. 5). RMSF values for CypA and CD147 in the CD147/CypA complex were indicated in Fig. 6a and b, respectively. RMSF values for CD147 in CD147/CypA complex were in the range of 3.5–4.5 nm. RMSF values for each TM/CD147 complex component were indicated in Fig. 7a and b for TM and CD147, respectively. RMSF values for CD147 in the TM/CD147 complex were in the range of 0.1–0.5 nm. The fluctuation of protein residues in the CD147/CypA and TM/CD147 complexes than a reference position had no undesired fluctuation during simulation time. RMSD values for MD simulation between TM peptide and CD147 were 0.8 to 1.2 nm after 50 ns stabilized (Fig. 8), indicating more stability of TM/CD147 than CD147/CypA. Molecular Mechanics/Poisson–Boltzmann Surface Area (MM/PBSA) method was used to compare the binding energy of two complexes CD147/CypA and TM /CD147 (Table 2). Based on the results, TM peptide has a high potential for binding to CD147 protein.

3.6. Interaction between TM peptide with DOPS-DOPC membrane

A DOPS-DOPC membrane model, including 80% DOPC and 20% DOPS membrane lipid, was constructed. For each lipid, 20 water molecule was added to the system, and the total lipids number was equal to 2000 molecules.

A coarse-grained simulation was conducted to examine the interaction of TM peptide with the DOPS-DOPC membrane. During 1500 ns CG model simulation, RMSD results displayed a stable conformation related to TM peptide structure inside membrane until

Table 1
Physicochemical properties of new analogues of hybrid peptide predicted by AntiCP server.

Peptide Sequence	Mutation position	Mol wt	pI	Net charge	hydrophobicity	hydrophilicity	Amphipathicity	SVMscore
GLPALISWIKRKQQGGGSRKKRRQRRR	0	3374.44	12.85	12.00	−0.62	0.93	1.36	0.67
ALPALISWIKRKQQGGGSRKKRRQRRR	1	3388.46	12.85	12.00	−0.62	0.91	1.36	0.82
CLPALISWIKRKQQGGGSRKKRRQRRR	1	3420.52	12.49	10.90	−0.62	0.90	1.36	0.82
DLPALISWIKRKQQGGGSRKKRRQRRR	1	3432.47	12.49	11.00	−0.65	1.04	1.36	0.82
HLPALISWIKRKQQGGGSRKKRRQRRR	1	3454.53	12.85	12.50	−0.64	0.91	1.41	0.80
NLPALISWIKRKQQGGGSRKKRRQRRR	1	3431.49	12.85	11.00	−0.65	0.94	1.36	0.81
ILPALISWIKRKQQGGGSRKKRRQRRR	1	3430.55	12.85	12.00	−0.60	0.87	1.36	0.83
SLPALISWIKRKQQGGGSRKKRRQRRR	1	3404.46	12.85	12.00	−0.64	0.94	1.36	0.82

Fig. 3. Docking results related to the interaction between hybrid peptide (TM) with CD147 protein in the specific binding site (proline 211). The blue, yellow and red colors are related to CD147 protein, TM peptide and the binding site in proline 211.

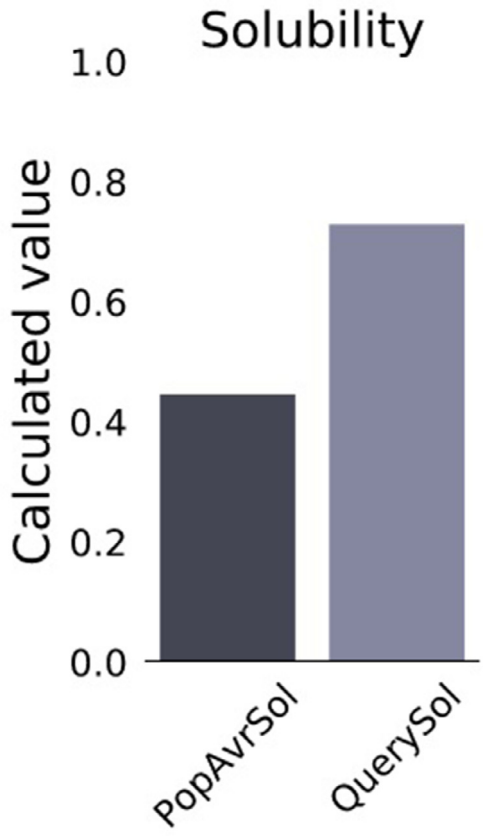

Fig. 4. The results related to solubility prediction by the protein-sol server (https://protein-sol.manchester.ac.uk). PopAvrSOL was selected as a template for solubility prediction.

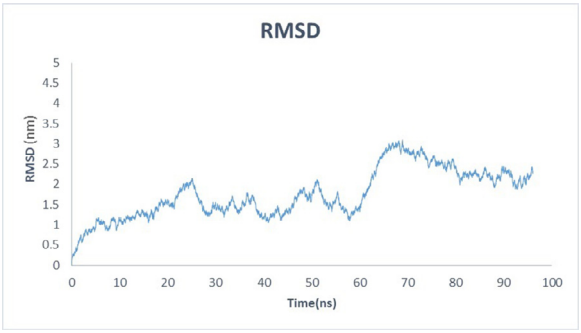

Fig. 5. RMSD values related to MD simulation done for Cyp A/CD147 interaction. The RMSD values were in the range of 0.4 to 3 nm during the simulation, and after time 70 ns remained stable.

the end of simulation time (Fig. 9). Based on the results, significant destruction was observed during the penetration of TM peptide into the membrane (Fig. 10). In this respect, tree figures (10a-10c) indicate the penetration of peptide into the membrane during 0 to 1500 ns simulations. In 0 ns simulation, the peptide is located out of the membrane (Fig. 10a). In 500 ns simulation, peptide is in contact with membrane surface (figue 10b) and finally in 1500 ns simulation, peptide has penetrated into membrane (Fig. 10c).

A partial density was also displayed during CG-MD simulation to indicate density distribution of the membrane and water along the z-axis during simulation (Fig. 11). While the start configuration was a mixture of membrane component and water, analysis of the density distribution of the membrane and water from the z-axis showed that the water and membrane have separated and water surrounds the membrane.

3.7. Analysis of peptide hydrophobicity

The peptide hydrophobicity was analyzed by the ProtScale program (The SIB Swiss Institute of Bioinformatics, Swiss) (http://www.expasy.ch/tools/protscale.html/) based on Kyte–Doolittle method (Hphob) [36]. The horizontal axis displayed the location of amino acids, and the vertical axis indicated the hydrophobicity rate, whose values above zero are related to hydrophobic amino acids in peptides (Fig. 12). Hydrophobicity analysis of peptide sequence by ProtScale tool displayed two individual hydrophobic parts (2–7 aa) and hydrophilic (10–15aa) properties related to Melittin in hybrid peptide hydrophobic part of Melittin have a role in deeper penetration of peptide to the inner part of the membrane. The C-terminal region of hybrid peptide (TAT) is rich in hydrophilic amino acids that play a role in attachment to the membrane's outer surface. In addition, based on the structure of the TAT peptide, the presence of the amino acids arginine and lysine has a strong interaction with the phosphate heads of the bilayer membrane, which leads to disruption of structure and penetration into the membrane.

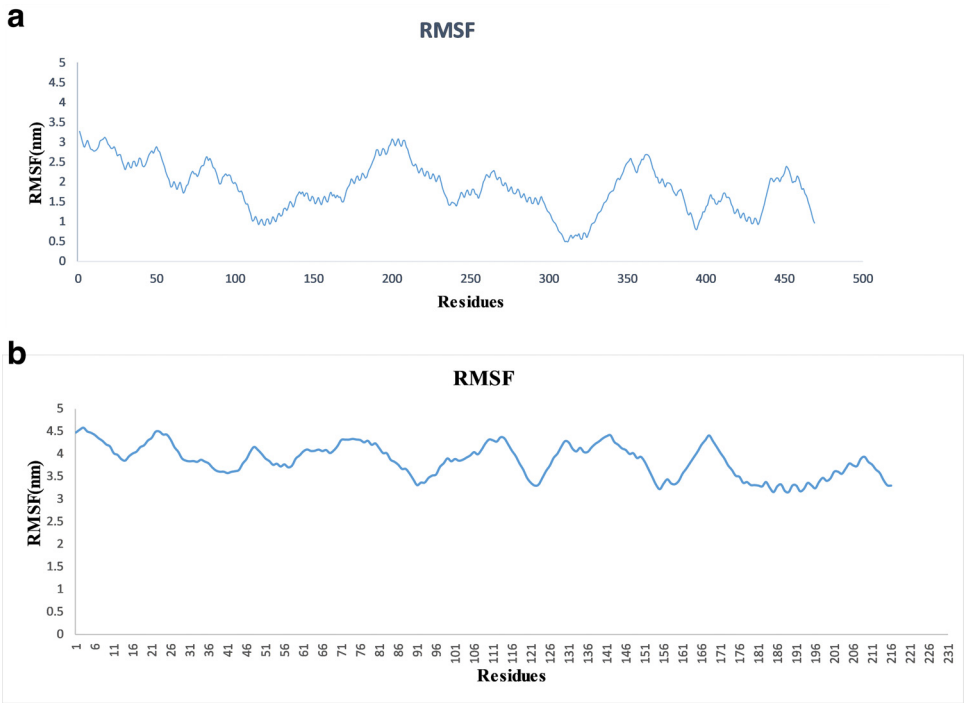

Fig. 6. RMSF results obtained from MD simulation performed for Cyp A /CD147 interaction. RMSF values were displayed for each component of the CD147/CypA complex during MD simulation. Fig. 6a and b indicate RMSF values of CypA and CD147, respectively. No undesired fluctuation was observed in the current simulation for Cyp A and CD147 proteins.

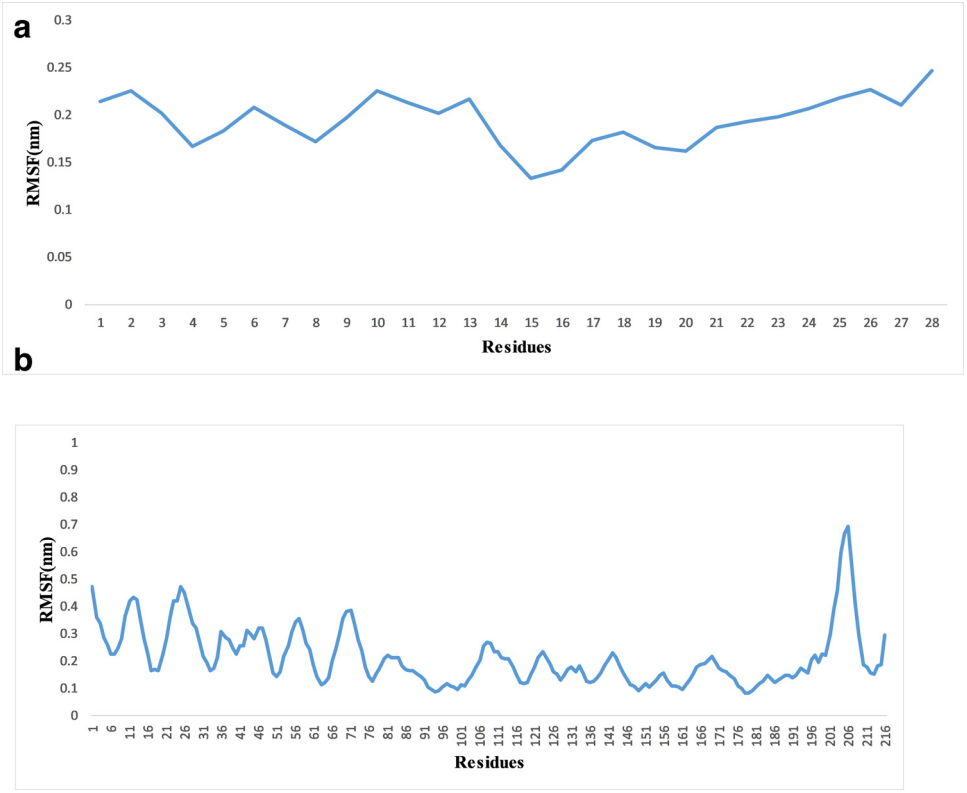

Fig. 7. RMSF results related to MD simulation for TM/CD147 interaction. Fig. 7a is related to TM peptide, and Fig. 7b is related to CD147. RMSF values indicate the fluctuation of protein residues over time from a reference position during simulation. There are no unwanted fluctuations for TM/ CD147 complex in the current simulation.

Table 2
The binding energy results during 100 ns MD simulation for CD147-CypA and TM-CD147 interactions.

Energy	CD147-CypA	TM-CD147
van der Waal energy	−516.612 +/- 27.538 kj/mol	−346.800 +/- 28.646 kj/mol
Electrostattic energy	−1849.649 +/- 106.725 kj/mol	−1069.632 +/- 41.093 kj/mol
Polar solvation energy	1326.222 +/- 106.895 kj/mol	879.497 +/- 57.964 kj/mol
SASA energy	−69.130 +/- 9.070 kj/mol	−42.517 +/- 1.567 kj/mol
SAV energy	0.000 +/- 0.000 kj/mol	0.000 +/- 0.000 kj/mol
WCA energy	0.000 +/- 0.000 kj/mol	0.000 +/- 0.000 kj/mol
Binding energy	−1109.169 +/- 130.575 kj/mol	−579.452 +/- 36.709 kj/mol

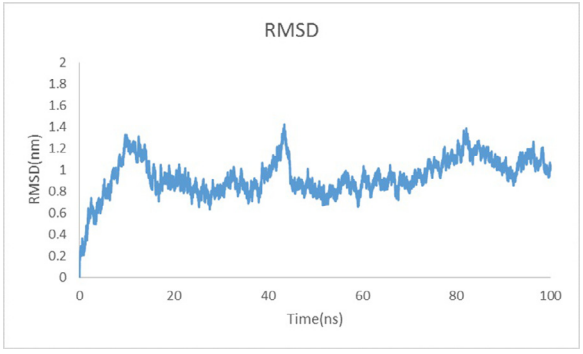

Fig. 8. RMSD values related to MD simulation done for TM/CD147 interaction. The RMSD values were in the range of 0.8 to 1.2 nm during the simulation, and after time 50 ns remained stable.

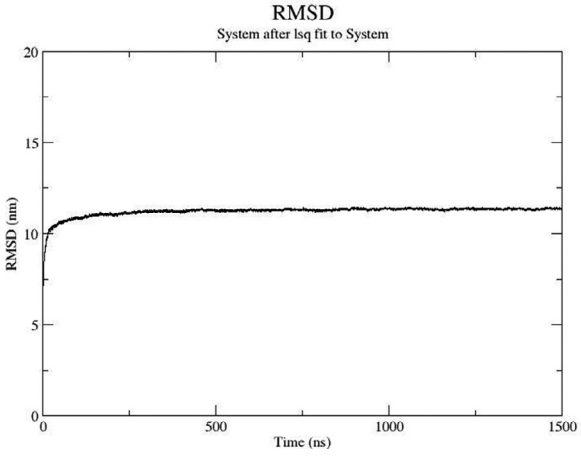

Fig. 9. During 1500 ns CG model simulation, RMSD results displayed a stable conformation related to TM peptide structure inside membrane until the end of simulation time.

4. Discussion

In addition to the critical role of CD147/ CypA in cancer, it has been documented that CD147 promotes virus infection via the interaction with the CypA molecule [37]. Hence, blocking of CD147/ CypA complex can be a promising therapeutic candidate for both cancer and COVID infection [15]. For instance, CD147-antagonist peptide 9 has an inhibitory effect on the entry of the COVID virus to host cells indicating the critical role of CD147 in promoting infection [37,38].

The recent promising outcomes regarding the anti-cancer properties of Melittin have made it an ideal candidate for cancer therapy. One of the critical mechanisms involved in the induction of apoptosis by Melittin is related to activating caspases by blocking the interaction between CypA to CD147 proteins [39]. The TAT peptide is a versatile cell-penetrating peptide for transferring a wide variety of therapeutic agents [20,40]. This study designed a dual hybrid peptide by combining melittin and TAT analogs. Based on bioinformatics results, two peptides indicated no negative interaction together spatially structure or biological activity. The anti-COVID19 and anti-cancer activities of the hybrid peptide(TM) could be related to blocking CypA / CD147 interaction coupled with a high penetration rate into tumor cells due to the existence of the TAT peptide. Studies indicate that 15 terminal amino acids of Melittin can act as an anti-cancer peptide [19]. In this study, the C-

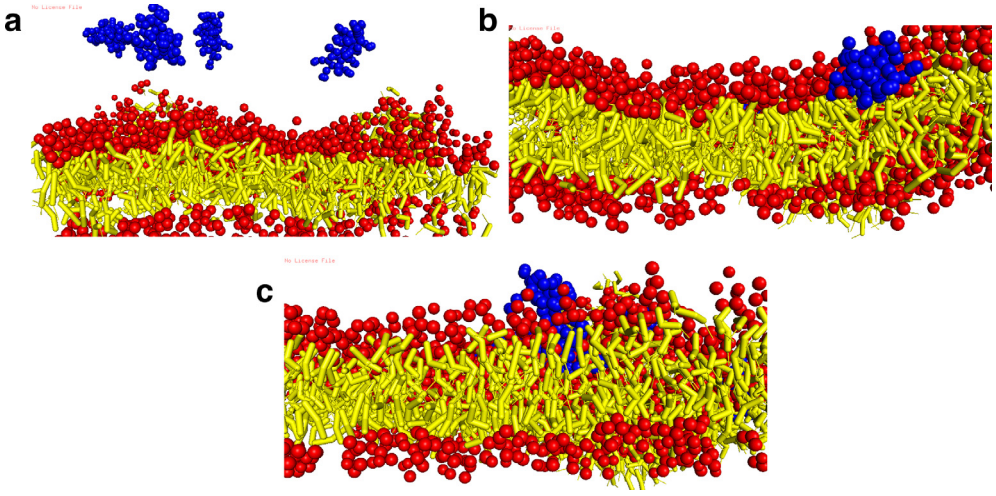

Fig. 10. The coarse-grained simulation for TM peptide interaction with DOPC/DOPS model membrane during 1500 ns. Fig. 10a: the peptide is out of the membrane in 0 ns simulation. Fig. 10b: the peptide is in contact with the membrane surface during 500 ns simulation. Fig. 10c: the peptide has penetrated the membrane in 1500 ns simulation. Peptide (blue) and lipid (yellow, red).

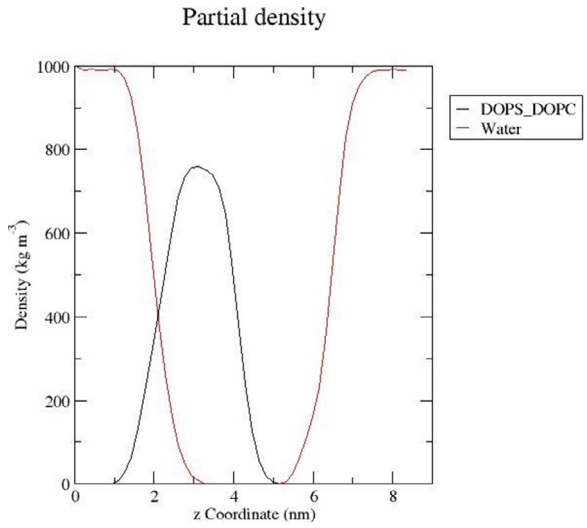

Fig. 11. Density distribution of the membrane and water along the z-axis during coarse-grained simulation was displayed by partial density plot.

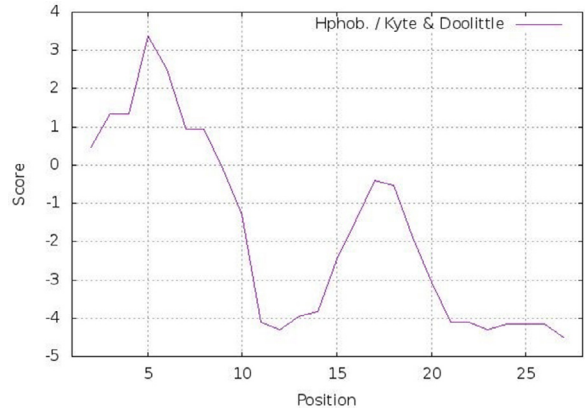

Fig. 12. Hydrophobicity analysis of peptide sequence was done by ProtScale tool. The horizontal axis indicates the location of the amino acids, and the vertical axis indicates hydrophobicity rate whose values above zero are related to hydrophobic amino acids in the peptide.

terminal portion of Melittin was fused to nine amino acids of TAT peptide by a suitable linker. Based on modeling and docking results, the GGGS linker can be a suitable selection for constructing TM peptide [27], and the resulting hybrid peptide was optimized by replacing glycine with serine in the sequence.

TM's stability and binding energy in the interaction with the CD147 receptor were predicted by MD simulation compared with the CypA and CD147 interaction. The high solubility and low toxicity of TM peptide was also predicted.

Until now, several studies have confirmed the penetration of Melittin into lipid membranes, such as the dioleoyl phosphatidylcholine (DOPC) bilayer [41,42].

According to RMSD and RMSF, the stability of the secondary structure of TM peptide in interaction with CD147 was confirmed. According to our findings, TM can be bound to CD147 with sufficient binding energy than the CD147-Cyp A protein complex.

Based on the results of CG-MD simulation, TM peptide has the potential for attaching to the DOPS / DOPC through its hydrophilic part and successfully entering the membrane through the hydrophobic part due to the permeability characteristic of TAT peptide. Based on physicochemical, MD and CG simulations results, the anti-cancer peptide designed can have a high potential for penetration into the lipid membrane. Therefore, the resulting peptide can be a suitable therapeutic candidate with high penetrating power into solid tumors.

5. Conclusion

In this study, the multifunctional inhibitory peptide could be an attractive therapeutic candidate to halter tumor types and COVID-19 infection.

Declarations

Author contributions

L.R. designed the study and performed the data analysis and interpretation; S.F. revised the manuscript. Z.M. and P.M wrote the first draft of the manuscript. E.Z.H. and N.KH discussed the results. Authors read and approved the final manuscript.

Funding

Not applicable.

Availability of data and materials

The datasets used and/or analyzed during the current study are available from the corresponding author on reasonable request.

Competing interests

The authors have no conflict of interest.

Ethics approval and consent to participate

The study was conducted after ethical approval of the ethics committee of Tabriz University of medical science, Tabriz Iran (**reference number:** IR.TBZMED.REC.1401.121 **(**.

Author statement

L.R. designed the study and performed the data analysis and interpretation; S.F. revised the manuscript. Z.M. and P.M wrote the first draft of the manuscript. E.Z.H. and N.KH discussed the results. Authors read and approved the final manuscript.

Declaration of Competing Interest

The authors declare that they have no known competing financial interests or personal relationships that could have appeared to influence the work reported in this paper.

The authors declare the following financial interests/personal relationships which may be considered as potential competing interests.

Data Availability

No data was used for the research described in the article.

Acknowledgments

This study was supported by the Infectious and Tropical Diseases Research Center, Tabriz University of Medical Sciences, Tabriz, Iran.

References

[1] A.L. Hilchie, D.W. Hoskin, M.R.P. Coombs, Anticancer activities of natural and synthetic peptides, Antimicrob.Peptides (2019) 131–147.
[2] E. Habermann, J. Jentsch, Sequence analysis of melittin from tryptic and peptic degradation products, Hoppe-Seyler's Z. Physiol. Chem. 348 (1) (1967) 37–50.
[3] M. Wachinger, A. Kleinschmidt, D. Winder, N. von Pechmann, A. Ludvigsen, M. Neumann, et al., Antimicrobial peptides melittin and cecropin inhibit replication of human immunodeficiency virus 1 by suppressing viral gene expression, J. Gen. Virol. 79 (4) (1998) 731–740.
[4] S.S. Saini, A.K. Chopra, J.W. Peterson, Melittin activates endogenous phospholipase D during cytolysis of human monocytic leukemia cells, Toxicon 37 (11) (1999) 1605–1619.
[5] G. Gajski, V. Garaj-Vrhovac, Bee venom induced cytogenetic damage and decreased cell viability in human white blood cells after treatment in vitro: a multi-biomarker approach, Environ. Toxicol. Pharmacol. 32 (2) (2011) 201–211.
[6] M. Akbarzadeh-Khiavi, M. Torabi, A.-.H. Olfati, L. Rahbarnia, A. Safary, Bio-nano scale modifications of melittin for improving therapeutic efficacy, Expert Opin Biol Ther (2022) just–accepted.
[7] G. Gajski, A.-.M. Domijan, B. Žegura, A. Štern, M. Gerić, I.N. Jovanović, et al., Melittin induced cytogenetic damage, oxidative stress and changes in gene expression in human peripheral blood lymphocytes, Toxicon 110 (2016) 56–67.
[8] X. Wu, B. Zhao, Y. Cheng, Y. Yang, C. Huang, X. Meng, et al., Melittin induces PTCH1 expression by down-regulating MeCP2 in human hepatocellular carcinoma SMMC-7721 cells, Toxicol. Appl. Pharmacol. 288 (1) (2015) 74–83.
[9] S. Farajnia, L. Rahbarnia, N. Khajehnasiri, H. Zarredar, Design of a hybrid peptide derived from Melittin and CXCL14–C17: a molecular dynamics simulation study, Biologia (2022) 1–12.
[10] P.J. Russell, D. Hewish, T. Carter, K. Sterling-Levis, K. Ow, M. Hattarki, et al., Cytotoxic properties of immunoconjugates containing melittin-like peptide 101 against prostate cancer: *in vitro* and *in vivo* studies, Cancer Immunol. Immunother.. 53 (5) (2004) 411–421.
[11] B. Li, W. Gu, C. Zhang, X.-.Q. Huang, K.-.Q. Han, C.-.Q. Ling, Growth arrest and apoptosis of the human hepatocellular carcinoma cell line BEL-7402 induced by melittin, Oncol. Res. Treat. 29 (8–9) (2006) 367–371.
[12] H. Hu, D. Chen, Y. Li, X. Zhang, Effect of polypeptides in bee venom on growth inhibition and apoptosis induction of the human hepatoma cell line SMMC-7721 in-vitro and Balb/c nude mice in-vivo, J. Pharm. Pharmacol. 58 (1) (2006) 83–89.
[13] L.C. Bordador, X. Li, B. Toole, B. Chen, J. Regezi, L. Zardi, et al., Expression of emmprin by oral squamous cell carcinoma, Int. J. Cancer 85 (3) (2000) 347–352.
[14] J. Wang, F. Li, J. Tan, X. Peng, L. Sun, P. Wang, et al., Melittin inhibits the invasion of MCF–7 cells by downregulating CD147 and MMP–9 expression, Oncol. Lett. 13 (2) (2017) 599–604.
[15] C. Liu, A. von Brunn, D. Zhu, Cyclophilin A and CD147: novel therapeutic targets for the treatment of COVID-19, Med. Drug Discov. 7 (2020) 100056.
[16] P.M. Taylor, R.J. Woodfield, M.N. Hodgkin, T.R. Pettitt, A. Martin, D.J. Kerr, et al., Breast cancer cell-derived EMMPRIN stimulates fibroblast MMP2 release through a phospholipase A 2 and 5-lipoxygenase catalyzed pathway, Oncogene 21 (37) (2002) 5765–5772.
[17] M. Moreno, E. Giralt, Three valuable peptides from bee and wasp venoms for therapeutic and biotechnological use: melittin, apamin and mastoparan, Toxins 7 (4) (2015) 1126–1150.
[18] B.C. Berks, F. Sargent, T. Palmer, The Tat protein export pathway, Mol. Microbiol. 35 (2) (2000) 260–274.
[19] H. Brooks, B. Lebleu, E. Vivès, Tat peptide-mediated cellular delivery: back to basics, Adv. Drug Deliv. Rev. 57 (4) (2005) 559–577.
[20] E. Virès, C. Granier, P. Prevot, B. Lebleu, Structure-activity relationship study of the plasma membrane translocating potential of a short peptide from HIV-1 Tat protein, Lett. Peptide Sci. 4 (4) (1997) 429–436.
[21] V. Yurchenko, S. Constant, E. Eisenmesser, M. Bukrinsky, Cyclophilin–CD147 interactions: a new target for anti-inflammatory therapeutics, Clin. Exp. Immunol. 160 (3) (2010) 305–317.
[22] T. Pushkarsky, V. Yurchenko, C. Vanpouille, B. Brichacek, I. Vaisman, S. Hatakeyama, et al., Cell surface expression of CD147/EMMPRIN is regulated by cyclophilin 60, J. Biol. Chem. 280 (30) (2005) 27866–27871.
[23] J. Schlegel, Cellular Receptors in cancer: CD147 and Mer: University of Colorado at Denver, Anschutz Medical Campus, 2012.
[24] M.K. Gill, Targeting cyclophilin-CD147 Interaction As an Approach to Treat Inflammatory Diseases, The George Washington University, 2009.
[25] X. Zhang, S. Sundram, T. Oppelstrup, S.I. Kokkila-Schumacher, T.S. Carpenter, H.I. Ingólfsson, et al., ddcMD: a fully GPU-accelerated molecular dynamics program for the Martini force field, J. Chem. Phys. 153 (4) (2020) 045103.
[26] M. Rizzuti, M. Nizzardo, C. Zanetta, A. Ramirez, S. Corti, Therapeutic applications of the cell-penetrating HIV-1 Tat peptide, Drug. Discov. Today 20 (1) (2015) 76–85.
[27] N. Rasafar, A. Barzegar, E.M. Aghdam, Design and development of high affinity dual anticancer peptide-inhibitors against p53-MDM2/X interaction, Life Sci. 245 (2020) 117358.
[28] J.C. Flores-Canales, M. Kurnikova, Targeting Electrostatic Interactions in Accelerated Molecular Dynamics with Application to Protein Partial Unfolding, J Chem Theory Comput. 11 (6) (2015) 2550–2559.
[29] B. Hess, C. Kutzner, D. Van Der Spoel, E. Lindahl, GROMACS 4: algorithms for highly efficient, load-balanced, and scalable molecular simulation, J. Chem. Theory Comput. 4 (3) (2008) 435–447.
[30] L.I. Vazquez-Salazar, M. Selle, A.H. De Vries, S.J. Marrink, P.C Souza, Martini coarse-grained models of imidazolium-based ionic liquids: from nanostructural organization to liquid–liquid extraction, Green Chem. 22 (21) (2020) 7376–7386.
[31] J. Xue, X. Huang, Y. Zhu, Using molecular dynamics simulations to evaluate active designs of cephradine hydrolase by molecular mechanics/Poisson–Boltzmann surface area and molecular mechanics/generalized Born surface area methods, RSC Adv. 9 (24) (2019) 13868–13877.
[32] Z.G. Qu, X.C. He, M. Lin, B.Y. Sha, X.H. Shi, T.J. Lu, et al., Advances in the understanding of nanomaterial–biomembrane interactions and their mathematical and numerical modeling, Nanomedicine 8 (6) (2013) 995–1011.
[33] E. Koren, A. Apte, R.R. Sawant, J. Grunwald, V.P. Torchilin, Cell-penetrating TAT peptide in drug delivery systems: proteolytic stability requirements, Drug Deliv. 18 (5) (2011) 377–384.
[34] X.-.L. Yu, T. Hu, J.-.M. Du, J.-.P. Ding, X.-.M. Yang, J. Zhang, et al., Crystal structure of HAb18G/CD147: implications for immunoglobulin superfamily homophilic adhesion, J. Biol. Chem. 283 (26) (2008) 18056–18065.
[35] S. Mahdian, M. Zarrabi, Y. Panahi, S. Dabbagh, Repurposing FDA-approved drugs to fight COVID-19 using in silico methods: targeting SARS-CoV-2 RdRp enzyme and host cell receptors (ACE2, CD147) through virtual screening and molecular dynamic simulations, Inf. Med. Unlocked 23 (2021) 100541.
[36] W.-.D. Zhang, H.-.X. Chen, Y.-.X. Wang, Z.-.P. Chen, Z.-.J. Shan, G. Xu, Bioinformatic analysis of c-Myc target from laryngeal cancer cell gene of laryngeal cancer, J. Cancer Res. Ther. 12 (1) (2016) 58.
[37] D.S. Hui, E. IA, T.A. Madani, F. Ntoumi, R. Kock, O. Dar, et al., The continuing 2019-nCoV epidemic threat of novel coronaviruses to global health - The latest 2019 novel coronavirus outbreak in Wuhan, China, Int. J. Infect. Dis. 91 (2020) 264–266.
[38] B. Manavalan, S. Basith, T.H. Shin, S. Choi, M.O. Kim, G. Lee, MLACP: machine-learning-based prediction of anticancer peptides, Oncotarget 8 (44) (2017) 77121.
[39] N. Oršolić, Bee venom in cancer therapy, Cancer Metastasis Rev. 31 (1) (2012) 173–194.
[40] F. Lv, J. Wang, H. Chen, L. Sui, L. Feng, Z. Liu, et al., Enhanced mucosal penetration and efficient inhibition efficacy against cervical cancer of PEGylated docetaxel nanocrystals by TAT modification, J. Controll. Release 336 (2021) 572–582.
[41] M. Bodescu, F. Rosenkötter, J. Fritz, Time lapse AFM on vesicle formation from mixed lipid bilayers induced by the membrane–active peptide melittin, Soft. Matter. 13 (38) (2017) 6845–6851.
[42] A.M. Feigin, J.H. Teeter, J.G. Brand, The influence of sterols on the sensitivity of lipid bilayers to melittin, Biochem. Biophys. Res. Commun. 211 (1) (1995) 312–317.